GRAVITATIONAL STRUCTURE UNDER MAJOR LUNAR BASINS. D. E. Smith[1], S. Goossens[2] and M. T. Zuber[1], [1]Dept. Earth, Atmospheric and Planetary Sciences, Massachusetts Institute of Technology, Cambridge, MA 02139 smithde@mit.edu, zuber@mit.edu, [2]Planetary Geology, Geophysics, and Geochemistry Laboratory, NASA Goddard Space Flight Center, Greenbelt, MD 20772 sander.j.goosens@nasa.gov.

Introduction: The gravity field of the Moon reflects the distribution of its mass. Although it is not possible to uniquely determine the mass distribution from gravity alone, the vertical component of gravity can provide information on the variation in density contrast with depth as a function of spherical harmonic degree. Further, a direct relationship between spherical harmonic degree and physical depth (km) using a simple point mass can provide an approximate (and relative) constraint on the depth distribution of density anomalies. Here we describe the structure under the Orientale basin from latitude 8º-32 º S along longitude 266 º E and show similar structures are present under the Imbrium and Smythii basins.

Approach: The gravity field at a point on the surface of a planet can be expressed as a series of spherical harmonics which describes the distribution of gravity as a function of spherical harmonic degree. The vertical component of gravity shows how gravity is distributed with depth where in general high degrees reflect mass variations that are close to the surface and lower degrees represent the mass distribution deeper in the crust or mantle. We show how the gravity varies with degree under large basins compared to areas between basins and those locations where the gravity field is near zero at the surface. We use the Bouguer gravity model 1200B [1] (Fig.1) derived from the free air gravity from GRAIL [2], and the topography from LRO/LOLA [3]

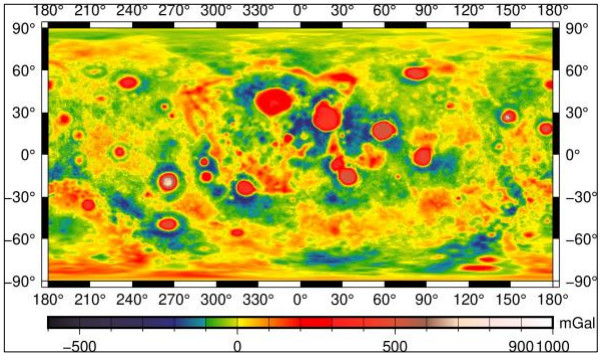

Fig. 1 *Lunar Bouguer gravity model 1200B [1] for degrees 6-600.*

To provide context for the structure seen in the radial gravity spectra we use a spherical harmonic degree to km relationship based upon a simple point mass model (pm-km) [4, 5] to indicate a possible depth range for a structure. However, we do not suggest that any observed structure can be fully represented as a point mass but can provide an indication of where a structure lies with respect to the lunar surface. No other data or model are employed in this investigation.

Basin Analysis: Figs. 2 & 3 collectively typify the gravity structure seen under all large impact basins. The figures show the Orientale basin Bouguer gravity field and 15 gravity spectra through the basin.

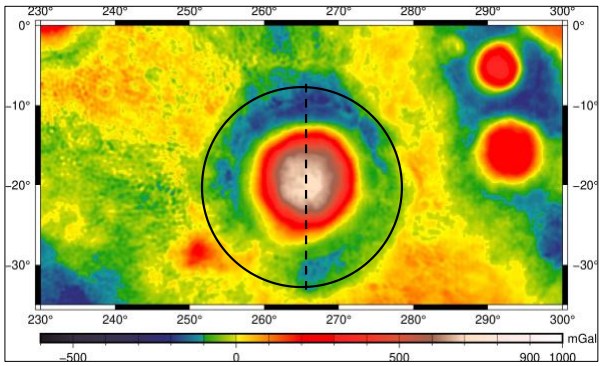

Fig. 2 Bouguer gravity field of *Orientale basin, degrees 6-600. Dashed vertical line, longitude 266 º from 8 º S to 32 º S, extends from the northern edge to the southern edge of the moat and analyzed in* Fig. 3.

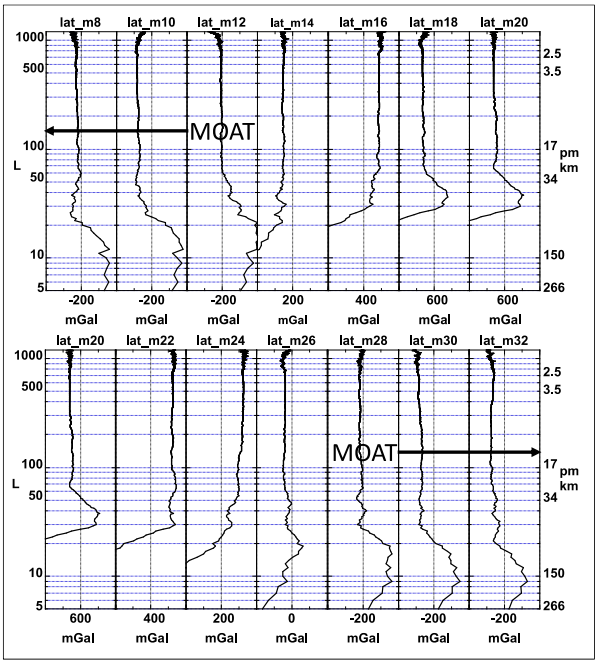

Fig. 3 *Gravity spectra spaced every 2 degrees across Orientale (dashed line, Fig. 2). Top, from the northern*

edge (8 ° S) of the moat to the center of the basin (20 ° S); lower, *from the center of the basin (20 ° S) to the southern edge (32 ° S) of the moat. Each spectrum has a width of 400 mGal with the center value identified. Nomenclature:* lat_m8 = 8 ° S.

The spectra show how the gravity structure changes under Orientale as the latitude changes from the northern edge of the moat, where the signal increases in magnitude, toward the central high (lat 20 ° S), and to the southern moat, where the signal again decreases. The depth as related to in pm-km of the maximum in any spectrum decreases to a minimum at the central high; for Orientale this is L~40, equal to 42 pm-km. The change from moat to central region is clearly shown in profiles 12 ° S and 14 ° S for L~40 where the magnitude changes from increasing to decreasing with depth. This variation of structure with location is seen under all large basins. Fig. 4 shows the gravity variations under Imbrium and Smythii on a single chart for each anomaly. Note: the moat is on the left in each figure and the central high is on the right.

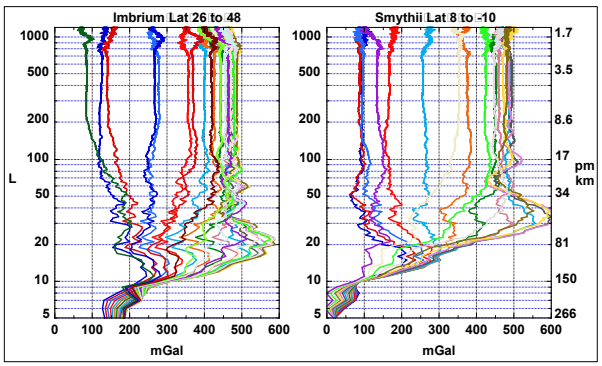

Fig. 4 *Gravity spectra under Imbrium and Smythii. The colored profiles are spaced at 1 degree of latitude and show how the magnitude of gravity in the basin varies with both latitude and spherical harmonic degree, L, and point-mass depth. Imbrium reaches a maximum at L~20 (*~80 pm-km, and Smythii at L~*35 (~48 pm-km). Orientale (Fig. 3) reached a maximum at L~40 (~42 pm-km).*

The three examples of the structure under major impact basins all have similar characteristics with a region of stable gravity from L~700-100 (2.5-17 pm-km) and a significant increase in magnitude at greater depth, L~40-20 (~42-80 pm-km). The upper stable region probably represents the upper crust that has been homogenized by impacts over billions of years [2]. The central region of larger gravity signal likely indicates an excess mass concentration as a result of melting, rebound and readjustment of the crust and mantle after the impact [6]. At the lowest level, L=20-10 (80-150 pm-km) all the profiles converge indicating the approximate depth at which the gravity field of the basin merges with the deeper interior at these degrees of L and pm-km.

Conclusion: The analysis of three prominent impact basins, Orientale, Imbrium and Smythii, shows how the vertical component of gravity under each basin varies systematically with location. The spherical harmonic degree, L, of the gravity maximum is an indication of the depth of the mass anomaly and a comparison with the depth of a point mass (pm-km) suggests the mass anomalies are within ~200 km of the surface.

Acknowledgments: GRAIL gravity data, 1200B gravity model, and LOLA topography are available in the Geosciences Node of the Planetary Data System (PDS).

References: [1] Goossens S. et al. (2020) *JGR Planets*, *125*, doi:10.1029/2019JE006086. [2] Zuber M. T. et al. (2013) *Science*, *399*, doi:10.1126/science.1231507. [3] Smith D. E. et al. (2016), *Icarus*, *283*, doi: 10.1016/j.icarus.2016.06.006 [4] Goossens, S. J. & Smith D. E. (2023) in revision. [5] Bowin C. (1983) *Marine Geodesy*, *7*, doi: 10.1080/15210608309379476. [6] Melosh H.J. et al. (2013) *Science*, *240*, doi: 10.1126/science.1235768.